Laser-assisted nuclear photoeffect

Anis Dadi[1] and Carsten Müller[1,2]
[1]*Max-Planck-Institut für Kernphysik, Saupfercheckweg 1, D-69117 Heidelberg, Germany*
[2]*Institut für Theoretische Physik I, Heinrich-Heine-Universität Düsseldorf, Universitätsstraße 1, D-40225 Düsseldorf, Germany*
(Received 17 April 2012; published 5 June 2012)

Proton emission from nuclei via the nuclear photoeffect in the combined electromagnetic fields of a γ-ray photon and an intense laser wave is studied. An S-matrix approach to the process is developed by utilizing methods known from the theory of nonperturbative laser-atom interactions. As a specific example, photo-proton ejection from halo nuclei is considered. We show that, due to the presence of the laser field, rich sideband structures arise in the photo-proton energy spectra. Their dependence on the parameters and relative orientation of the photon fields is discussed.

DOI: 10.1103/PhysRevC.85.064604 PACS number(s): 25.20.Dc, 32.80.Wr, 42.55.Vc

I. INTRODUCTION

Studies of the nuclear photoeffect have provided important insights into the structure of the nucleus. The research field was opened with the experiments by Chadwick and Goldhaber on the photodisintegration of the deuteron where γ rays from a radioactive source were utilized [1]. Systematic investigations of the nuclear photoeffect were carried out by Bothe and Gentner, which relied on high-energy γ rays produced with the aid of an accelerator [2]. Modern experiments on photonuclear reactions typically apply energetic photons from synchrotron radiation, electron bremsstrahlung, or Compton backscattering sources [3].

Due to an enormous and still ongoing technological progress during the last two decades, intense photon beams from powerful laser sources are emerging nowadays into a novel tool for photonuclear studies [4]. For example, a facility devoted particularly to laser-nuclear physics is currently being constructed as part of the Extreme Light Infrastructure project [5,6].

Direct interactions of laser fields and nuclei are usually very weak because of the large mismatch between the relevant energy scales. Typically, the laser photon energy as well as the electric work performed by the laser field over the nuclear extension are by orders of magnitude smaller than the nuclear level spacing [7]. Indirect laser-nucleus coupling schemes have therefore mostly been considered, which are mediated by secondary particles such as electrons. Prominent examples are nuclear reactions in laser-produced plasmas [4,8] where, in particular, photofission and photoneutron production through high-energy bremsstrahlung by laser-accelerated electrons have been observed [9]. Besides, theoreticians have investigated laser-assisted internal conversion [10], nuclear reactions via electron-bridge mechanisms [7,11], and nuclear Coulomb excitation in laser-driven atoms [12]. A possibility of lifetime measurements on short-lived excited levels in proton-rich isotopes via laser-driven streaking of emitted protons has been proposed [13]. In view of the ever increasing available laser intensities as well as frequencies, prospects for direct laser-induced nuclear reactions are nowadays also being explored. Resonant photoexcitation of nuclear transitions may occur when an intense x-ray laser pulse interacts with a counterpropagating nuclear beam of moderately relativistic energy [14]. Laser-induced dynamic nuclear Stark shifts [15] and excitation of nuclear giant dipole resonances [16] have been examined as well.

Apart from laser-induced reactions, also laser-assisted processes are of interest. These are processes that can already occur without the presence of a laser field but may be modified when a laser field is present. Examples are the laser-assisted internal conversion [10] and the laser-assisted nuclear excitation by electron transition [11] mentioned above. In general, the requirements on the laser field parameters in order to cause a sizable effect are substantially less demanding for laser-assisted than for direct laser-induced nuclear processes.

Laser-assisted processes have been studied thoroughly in atomic physics. They comprise, for instance, laser-assisted scattering of x-rays, electrons, and ions on atomic targets [17–19]. In particular, the laser-assisted photoelectric effect in atoms has been investigated intensively [20]. Characteristic modifications of the photoelectron spectra due to the presence of the laser field have been found. Corresponding experimental studies [21] have been rendered feasible in recent years by the availability of synchronized optical and extreme-ultraviolet (XUV) beams, with the latter being produced by free-electron lasers or high-harmonic generation. The inverse of the laser-assisted atomic photoeffect is laser-assisted radiative recombination of electrons with ions [22].

In the present paper we consider the laser-assisted nuclear photoeffect. That is, photo-proton emission from a nucleus, which is subject to the combined electromagnetic fields of a γ photon and an intense laser beam. We assume that the γ-photon energy exceeds the proton separation energy, $\omega_\gamma > E_b$, and study modifications of the γ-induced proton emission in the presence of an intense laser field of relatively low frequency, $\omega_0 \ll E_b$. Regarding the nuclear species, we focus our consideration on one-proton halo nuclei because they possess low proton separation energies [23–26]. Moreover, their structure allows us to develop a theoretical treatment of the photo-proton emission, which is similar to laser-assisted photoionization in atoms [20,22]. Symbolically, the process under investigation may be written as

$$ {}^{A}_{Z}[Xp] + \omega_\gamma + n\omega_0 \longrightarrow {}^{A-1}_{Z-1}[X] + {}^{1}_{1}p, \tag{1}$$

where n denotes the number of laser photons involved. We shall show that the assistance by the laser field may have a substantial impact on the photo-proton energy spectra, which are significantly broadened and obtain a rich structure.

The paper is organized as follows. In Sec. II we derive the quantum mechanical amplitude for the laser-assisted photoeffect in halo nuclei. The strong-field approximation will be used, describing the emitted photo-proton in the laser field by a Volkov state. An analytical expression for the cross section of the process is given, which involves a summation over the number n of participating laser photons. Our numerical results are presented in Sec. III, which demonstrate the characteristic influence exerted by the assisting laser field on the photo-proton emission. The physical origin of the various effects is discussed and their dependencies on the parameters of the photon fields and their relative orientation is analyzed. We conclude with a brief summary and outlook in Sec. IV.

Natural units with $\hbar = c = \varepsilon_0 = 1$ are used throughout unless otherwise stated.

II. THEORETICAL FRAMEWORK

In this section, we develop a theoretical model to describe the nuclear photoeffect by an incident γ photon in the presence of a background laser field. Our approach is inspired by existing theoretical treatments of laser-assisted photoionization of atoms [20,22]. We will restrict the consideration to halo nuclei with a weakly bound outer proton because this exotic nuclear species possesses low proton separation energies.

The laser field is assumed to be a circularly polarized, monochromatic wave of frequency ω_0. It is described by the time-dependent vector potential

$$\vec{A}_L(t) = A_0[\cos(\omega_0 t)\,\vec{e}_1 + \sin(\omega_0 t)\,\vec{e}_2], \tag{2}$$

with amplitude A_0. The corresponding amplitude of the laser electric field is $F_0 = \omega_0 A_0$. The unit vectors $\vec{e}_j$ $(j = 1, 2)$ are orthogonal to each other, $\vec{e}_1 \cdot \vec{e}_2 = 0$. Note that in Eq. (2) the dipole approximation has been applied, which disregards the spatial field dependence. This approximation is well justified because, for the laser parameters under consideration, the scale of the spatial field variations—which is set by the laser wavelength $\lambda_0 = 2\pi/\omega_0$—is much larger than both the nuclear size a_0 and the laser-driven excursion amplitude $\ell_0 \sim eF_0/(m\omega_0^2)$ of the emitted proton in the continuum; m denotes the proton mass. Hence, the proton experiences a field that is quasiconstant in space.

A. Derivation of S matrix

The Hamiltonian describing the evolution of the halo proton in the combined fields of the laser beam, the γ photon, and the nuclear core reads

$$H = \frac{1}{2m}(\hat{\vec{p}} - e\vec{A}_L(t) - e\vec{A}_\gamma(\vec{r}, t))^2 + V_{\rm nuc}(r)\,. \tag{3}$$

Here, $\hat{\vec{p}} = -i\vec{\nabla}$ is the momentum operator of the proton, e the proton charge, and $V_{\rm nuc}$ the potential of the nuclear core. Besides, the vector potential of the incident γ photon with energy ω_γ, momentum $\vec{k}_\gamma$, and polarization vector $\vec{\varepsilon}$ is

$$\vec{A}_\gamma(\vec{r}, t) = \sqrt{\frac{2\pi}{V_\gamma \omega_\gamma}}\, e^{i(\vec{k}_\gamma \cdot \vec{r} - \omega_\gamma t)}\,\vec{\varepsilon}\,, \tag{4}$$

within the normalization volume V_γ. The relevant interaction Hamiltonian contained in Eq. (3), which is responsible for γ-photon absorption by the nucleus, is given by

$$H_{\rm int} = -\frac{e}{m}(\hat{\vec{p}} - e\vec{A}_L(t)) \cdot \vec{A}_\gamma(\vec{r}, t)\,. \tag{5}$$

It can lead to the ejection of the halo proton from the nucleus into the continuum.

The corresponding S matrix is of the general form

$$S_{fi} = -i\int_{-\infty}^{\infty} \langle \Psi_f | H_{\rm int} | \Psi_i^{(+)} \rangle\, dt\,. \tag{6}$$

Here, $\Psi_i^{(+)}$ denotes a state of the full Hamiltonian (3), whereas Ψ_f is a state of the unperturbed Hamiltonian $H_0 = \frac{1}{2m}[\hat{\vec{p}} - e\vec{A}_L(t)]^2 + V_{\rm nuc}(r)$, lacking the interaction with the γ-photon field. However, even for the unperturbed problem, the exact form of the corresponding wave function in Eq. (6) is not known since H_0, containing both the laser vector potential and the nuclear potential, is nontrivial. Suitable approximations to describe the initial and final proton states are thus needed.

First we note that the influence of the γ-photon field on the initial proton wave function may be disregarded since it is assumed to represent a small perturbation. Besides, the laser field will also exert only a minor influence on the halo proton in the initial state due to its tight binding to the nuclear core. Consequently, the exact initial state $\Psi_i^{(+)}$ in Eq. (6) may be approximated by a stationary field-free wave function in the nuclear potential $V_{\rm nuc}$,

$$\Psi_i^{(+)}(\vec{r}, t) \approx \phi_0(\vec{r})\, e^{iE_b t}, \tag{7}$$

with the nuclear binding energy $-E_b$. Assuming that the halo proton is in an s state, the space-dependent part can be expressed approximately in Yukawa form as [24]

$$\phi_0(\vec{r}) = \frac{c_0}{\sqrt{4\pi}}\,\frac{e^{-\beta r}}{\beta r}\,, \tag{8}$$

with $\beta = \nu\sqrt{2mE_b}$, where ν is a free parameter of order unity, which is adjusted to reproduce the measured value of the halo root-mean-square radius. The normalization constant, guaranteeing that $\langle \phi_0 | \phi_0 \rangle = 1$, amounts to $c_0 = \sqrt{2\beta^3}$. We point out that the approximation of the wave function in Eq. (8) is not unique. But, according to Hartree-Fock calculations [27], it is appropriate for describing the main halo properties such as the large spatial extension of the halo-proton density.

Second, when the energy of the ejected proton is relatively high (as compared with the nuclear binding energy), the core potential will have a rather small effect on the final proton state in the continuum. The influence of the laser field on this state, however, may be substantial and cannot be ignored. In the relevant Hamiltonian H_0 we may therefore drop the nuclear potential, keeping only the interaction with the laser field. Consequently, the final state may be approximated by a Volkov state, $\Psi_f(\vec{r}, t) \approx \psi_{\vec{p}}(\vec{r}, t)$, which exactly accounts for

the interaction of the laser field with the ejected proton. It is a solution to the time-dependent Schrödinger equation

$$i\frac{\partial}{\partial t}\psi_{\vec{p}}(\vec{r},t) = \frac{1}{2m}(\hat{\vec{p}} - e\vec{A}_L(t))^2\psi_{\vec{p}}(\vec{r},t) \tag{9}$$

and reads

$$\psi_{\vec{p}}(\vec{r},t) = \frac{e^{i\vec{p}\cdot\vec{r}}}{\sqrt{V}}\exp\left\{-\frac{i}{2m}\int_{t_0}^{t}[\vec{p} - e\vec{A}_L(t')]^2 dt'\right\}. \tag{10}$$

Here, $\vec{p}$ denotes the proton momentum outside the field and V is a normalization volume. Note that the lower integration boundary t_0 gives rise to an immaterial constant phase factor, which may be dropped.

The approximations applied to describe the initial and final states are known in atomic physics as strong-field approximation (SFA). The S matrix of Eq. (6) thus becomes $S_{fi} \approx S_{\vec{p}\,0}$, with

$$S_{\vec{p}\,0} = \frac{ie}{m}\sqrt{\frac{2\pi}{V_\gamma\omega_\gamma}}\int dt\int d^3r\ \psi^*_{\vec{p}}(\vec{r},t) \times(\vec{p} - e\vec{A}_L)\cdot\vec{\varepsilon}\, e^{i(\vec{k}_\gamma\cdot\vec{r}-\omega_\gamma t)}\phi_0(\vec{r})\, e^{iE_b t}. \tag{11}$$

B. Analytical evaluation of S matrix

The strong-field approximated S matrix in Eq. (11) can be evaluated by analytical means. In view of the temporal integral we note that, by inserting Eq. (2) into Eq. (10) and evaluating the integrals in the exponent, the Volkov state of the photo-proton may be written, after complex conjugation, as

$$\psi^*_{\vec{p}}(\vec{r},t) = \frac{e^{-i\vec{p}\cdot\vec{r}}}{\sqrt{V}}\exp\left[i\left(\frac{p^2}{2m} + U_\mathrm{p}\right)t\right] f(t), \tag{12}$$

with the time-dependent periodic function

$$f(t) = \exp\left[-i(\alpha_1\sin\omega_0 t - \alpha_2\cos\omega_0 t)\right]. \tag{13}$$

Here, we have introduced the abbreviation

$$\alpha_j = \frac{eF_0}{m\omega_0^2}p_j\,, \tag{14}$$

with $p_j = \vec{p}\cdot\vec{e}_j$ $(j = 1, 2)$. Besides, the ponderomotive energy of the photo-proton is given by

$$U_\mathrm{p} = \frac{e^2F_0^2}{2m\omega_0^2}. \tag{15}$$

It represents the cycle-averaged kinetic energy of the proton in the laser field.

We note that $f(t)$ may also be written as

$$f(t) = \exp\left[-i\alpha\sin(\omega_0 t - \eta_0)\right], \tag{16}$$

with $\alpha = \sqrt{\alpha_1^2 + \alpha_2^2}$ and $\eta_0 = \arctan(\alpha_2/\alpha_1)$. By exploiting the Jacobi-Anger identity [28], we can expand $f(t)$ into Fourier series

$$f(t) = \sum_{n=-\infty}^{+\infty} B_n\, e^{-in\omega_0 t}\,, \tag{17}$$

with the Fourier coefficients given by $B_n = J_n(\alpha)e^{in\eta_0}$, where J_n is a Bessel function of the first kind of integer order n. Similarly, we find

$$\cos(\omega_0 t)f(t) = \sum_{n=-\infty}^{+\infty} C_n\, e^{-in\omega_0 t}\,,$$
$$\sin(\omega_0 t)f(t) = \sum_{n=-\infty}^{+\infty} D_n\, e^{-in\omega_0 t}\,, \tag{18}$$

with

$$C_n = \tfrac{1}{2}[J_{n+1}(\alpha)e^{i(n+1)\eta_0} + J_{n-1}(\alpha)e^{i(n-1)\eta_0}],$$
$$D_n = \tfrac{1}{2i}[J_{n+1}(\alpha)e^{i(n+1)\eta_0} - J_{n-1}(\alpha)e^{i(n-1)\eta_0}]. \tag{19}$$

Hence, the S matrix (11) adopts the form

$$S_{\vec{p}\,0} = \frac{ie}{m}\sqrt{\frac{2\pi}{VV_\gamma\omega_\gamma}}\sum_{n=-\infty}^{+\infty}\mathcal{M}_n\int d^3r e^{-i(\vec{p}-\vec{k}_\gamma)\cdot\vec{r}}\,\phi_0(\vec{r}) \times\int dt e^{i(\frac{p^2}{2m}+U_\mathrm{p}+E_b-\omega_\gamma-n\omega_0)t}\,. \tag{20}$$

Here, we introduced

$$\mathcal{M}_n = \vec{\varepsilon}\cdot\vec{p}\,B_n - eA_0\varepsilon_1\,C_n - eA_0\varepsilon_2\,D_n, \tag{21}$$

with $\varepsilon_j = \vec{\varepsilon}\cdot\vec{e}_j$ $(j = 1, 2)$.

From Eq. (20) it becomes transparent that the time integral will result in a δ function, which ensures energy conservation in the process. Further, the space integral produces the Fourier transform of the bound halo state. By setting $\vec{q} = \vec{p} - \vec{k}_\gamma$, it reads

$$G(q) = \int d^3r e^{-i\vec{q}\cdot\vec{r}}\,\phi_0(\vec{r}) = \frac{2\sqrt{\pi}\,c_0}{\beta(\beta^2+q^2)}\,. \tag{22}$$

We finally obtain the following expression for the S matrix

$$S_{\vec{p}\,0} = \frac{ie}{m}\frac{(2\pi)^{3/2}}{\sqrt{VV_\gamma\omega_\gamma}}\sum_{n=n_0}^{+\infty}\mathcal{M}_n\,G(|\vec{p}-\vec{k}_\gamma|) \times\delta\left(\frac{p^2}{2m} + U_\mathrm{p} + E_b - \omega_\gamma - n\omega_0\right), \tag{23}$$

where n_0 represents the smallest integer that is in accordance with the energy conservation condition. The δ function fixes, for each laser photon number n, the absolute value of the emitted proton momentum at

$$p_n = \sqrt{2m(\omega_\gamma + n\omega_0 - U_\mathrm{p} - E_b)} \tag{24}$$

(i.e., n_0 is the smallest integer which leads to a positive value of the expression under the root).

C. Photonuclear cross section

The total cross section for the laser-assisted nuclear photoeffect is obtained by squaring the S matrix in Eq. (23), integrating over the final proton momentum, and dividing out the γ-photon flux $j = 1/V_\gamma$ and a unit time T

$$\sigma = \frac{1}{jT}\int\frac{Vd^3p}{(2\pi)^3}\,|S_{\vec{p}\,0}|^2\,. \tag{25}$$

In accordance with the summation over the number of exchanged laser photons in Eq. (23), also the total cross section decomposes

$$\sigma = \sum_{n=n_0}^{+\infty} \sigma_n \tag{26}$$

into a sum over partial cross sections σ_n. They are given by

$$\sigma_n = \frac{e^2}{2m\omega_\gamma} \int_0^\pi d\theta \int_0^{2\pi} d\phi p_n \mathcal{M}_n^2 G(|\vec{p}_n - \vec{k}_\gamma|)^2 \tag{27}$$

with $\vec{p}_n = p_n(\sin\theta\cos\phi, \sin\theta\sin\phi, \cos\theta)$. Due to the energy-conserving δ function in Eq. (23), the computation of the partial cross section reduces to an integration over the emission angles of the photo-proton, which can be carried out by numerical means.

III. NUMERICAL RESULTS AND DISCUSSION

Based on Eqs. (26) and (27), we have performed numerical calculations of the laser-assisted nuclear photoeffect in halo nuclei. In what follows, we will consider throughout the one-proton halo isotope ^{8}B [23–25]. It has a lifetime of about 770 ms and may, thus, be considered stable on the femtosecond to nanosecond time scales of intense laser pulses. The proton separation energy is very low and amounts to $E_b = 137$ keV [24]. For the root-mean-square distance in the ^{7}Be-proton system we employ the value $R_{\rm rms} \approx 4.73$ fm [25] and, accordingly, set $\nu = 1.84$ in Eq. (8).

The incident γ photon is assumed to have a relatively high energy of $\omega_\gamma = 3$ MeV in order to guarantee that the nuclear core potential $V_{\rm nuc}$ in Eq. (3) has a rather small influence on the proton in the continuum. The γ photon propagates into the x direction and is polarized along the z axis, $\vec{\varepsilon} = \vec{e}_z$. We note that γ photons of several MeV energy can be produced today through bremsstrahlung of laser-accelerated electron bunches [29]. An experimental setup to probe the laser-assisted nuclear photoeffect could therefore rely on two sources of intense laser radiation: one to generate the γ rays and the second one to provide the assisting laser field.

Several laser frequencies in the XUV and x-ray domains with various intensities have been applied in order to reveal the dependence of the process on these parameters. The polarization vectors of the laser field have almost always been chosen as $\vec{e}_1 = \vec{e}_y$ and $\vec{e}_2 = \vec{e}_z$ [see Eq. (2)]. Hence, the polarization vector of the γ photon lies in the polarization plane of the circularly polarized laser field. Additionally, in Sec. III C another polarization plane of the laser is considered in order to study the relevance of the field geometry.

We briefly comment on the current status of high-intensity laser sources operating in the XUV and x-ray regimes. The FLASH facility (DESY, Germany), which is based on a free-electron laser, produces brilliant photon beams with XUV frequencies of $\omega_0 \sim 100$ eV at peak intensities up to $\sim 10^{17}$ W/cm^2 [30]. The free-electron laser at the Linac Coherent Light Source (SLAC, Stanford) is presently able to generate x-ray photon beams with $\omega_0 \sim 1$ keV at $\sim 10^{18}$ W/cm^2 [31]. A substantial further increase of the attainable peak intensities is envisaged at both facilities. High-intensity coherent XUV and x-ray pulses can also be created through harmonic emission from laser-irradiated plasma surfaces [32].

A. Transition from perturbative to nonperturbative laser-proton coupling

Figure 1 shows the partial cross sections σ_n as a function of the number n of emitted ($n < 0$) or absorbed ($n > 0$) laser photons. The laser frequency lies in the x-ray domain and amounts to $\omega_0 = 2$ keV. The laser intensity varies between $\sim 10^{21}$–10^{24} W/cm^2. Note that the distributions shown in Fig. 1 reflect the energy spectra of the emitted proton: at a given value of n, the proton energy is $E_n = \omega_\gamma + n\omega_0 - U_{\rm p} - E_b$. The fraction of protons with this energy amounts to σ_n/σ.

In the absence of a laser field, the photo-proton energy spectrum would consist of a single line located at $\omega_\gamma - E_b \approx 2.86$ MeV. As Fig. 1 illustrates, the presence of the laser field leads to sidebands in the energy distribution which surround the central line and are equally spaced by a laser photon energy ω_0.

When the laser intensity is relatively low, only the first few sidebands show up [see Fig. 1(a)]. Their height, as compared with the central line, is suppressed because the laser-proton interaction represents here a small perturbation only. The expansion parameter of the corresponding perturbation series is given by

$$\alpha_{\rm max} = \frac{eF_0 p_{\rm max}}{m\omega_0^2} \tag{28}$$

where $p_{\rm max}$ denotes the maximum value of the photo-proton momentum component in the polarization plane of the laser field. It enters into the partial cross section σ_n as maximum argument of the Bessel function $J_n(\alpha)$. Since $J_n(x) \approx \frac{1}{n!}(\frac{x}{2})^n$ for $x \ll 1$ at $n \geqslant 0$ and $J_{-n}(x) = (-1)^n J_n(x)$ [28], higher photon orders are suppressed when the expansion parameter is small. In particular, the first and second sidebands visible in Fig. 1(a) are reduced by relative factors of $\sigma_{\pm1}/\sigma_0 \sim \alpha_{\rm max}^2/4 \sim 0.05$ and $\sigma_{\pm2}/\sigma_0 \sim \alpha_{\rm max}^4/8 \sim 10^{-3}$, as compared with the central line.

We point out that the square of $\alpha_{\rm max}$, which enters into the series expansion, contains the fine-structure constant e^2 as well as a laser-intensity-dependent factor. This is in agreement with the form of the expansion parameter derived in [33], where a general analysis of the convergence properties of perturbative series expansions in strong-field laser physics has been performed. Besides, in the present situation, $\alpha_{\rm max}$ contains a factor of $p_{\rm max}$, which depends on the difference between the γ-photon energy ω_γ and the nuclear binding energy E_b. In fact, all three interactions in the Hamiltonian (3) are reflected in the structure of the expansion parameter (28).

As Fig. 1(b) shows, when the laser intensity is increased, the number of sidebands grows. Besides, the contribution from the sidebands to the total cross section (26) can be comparable to or even exceed the contribution from the central line. When the laser intensity is increased even further, an extended plateau of sidebands of similar height arises [see Fig. 1(c)].

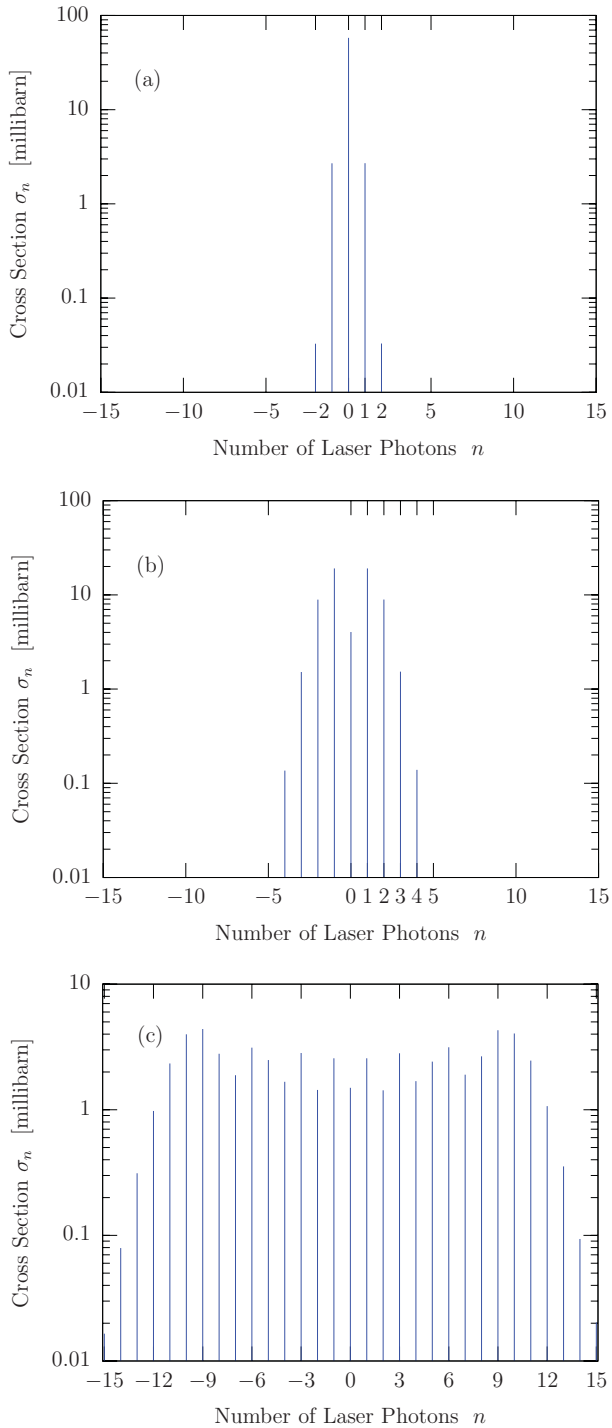

FIG. 1. (Color online) Distributions of the partial cross sections σ_n for laser-assisted proton emission from ^{8}B, as a function of the number of absorbed ($n > 0$) or emitted ($n < 0$) laser photons. The circularly polarized laser field has a frequency of $\omega_0 = 2$ keV. Its intensity amounts to (a) $I = 4.0 \times 10^{21}$ W/cm^2, (b) $I = 1.0 \times 10^{23}$ W/cm^2, and (c) $I = 2.5 \times 10^{24}$ W/cm^2, respectively. The γ-ray photon has an energy of $\omega_\gamma = 3$ MeV; its polarization vector lies in the polarization plane of the laser.

Here, the value of the coupling parameter (28) has raised to $\alpha_{\max} \approx 2.4$, indicating that a transition from perturbative to nonperturbative laser-proton coupling has occurred. In terms of the photo-proton energy, the plateau covers the range from about 2.84 MeV to 2.88 MeV. Note that the value of the ponderomotive energy is small, $U_p \approx 2$ eV.

We point out that the total cross section in Figs. 1(a)–1(c) is always the same, $\sigma = \sum_n \sigma_n \approx 63.4$ mb. Hence, while the presence of the laser field distributes the photo-proton energies over a broad range, it does not affect the total probability of the process. For comparison we note that an estimate of the total cross section based on the Bethe-Peierls formula [34] yields a value of about 20 mb and, thus, agrees with the prediction from our model by the order of magnitude.

B. Fully nonperturbative laser-proton interaction

In Section III A we have seen that the coupling between the emitted proton and the x-ray laser field becomes stronger when the laser intensity is enhanced. By inspection of the coupling parameter (28) we may expect that the interaction strength grows further when the laser frequency is decreased. This is confirmed in Fig. 2 where the distribution of the partial cross sections σ_n is displayed at an XUV laser frequency of $\omega_0 = 100$ eV and a field intensity of $I = 6.25 \times 10^{21}$ W/cm^2 (and otherwise unchanged parameters). The laser-proton interaction exhibits a highly nonperturbative character now, which is related to a large value of the coupling parameter, $\alpha_{\max} \approx 238$. A multitude of sidebands appear, forming a quasicontinuous distribution and featuring several maxima whose height is growing toward the side wings. Hence, the γ-induced proton emission proceeds most likely with the simultaneous absorption or emission of hundreds of laser photons. The cutoff of the distribution at $|n| \gtrsim 240$ may be traced back to the properties of the Bessel functions $J_n(\alpha)$ of large order, which quickly approach zero in the region where $|n| > \alpha$ [28]. The proton energy varies between 2.84 MeV and 2.88 MeV, accordingly.

The width of the distribution in Fig. 2 can be understood by a classical-physics consideration. Let us consider a proton

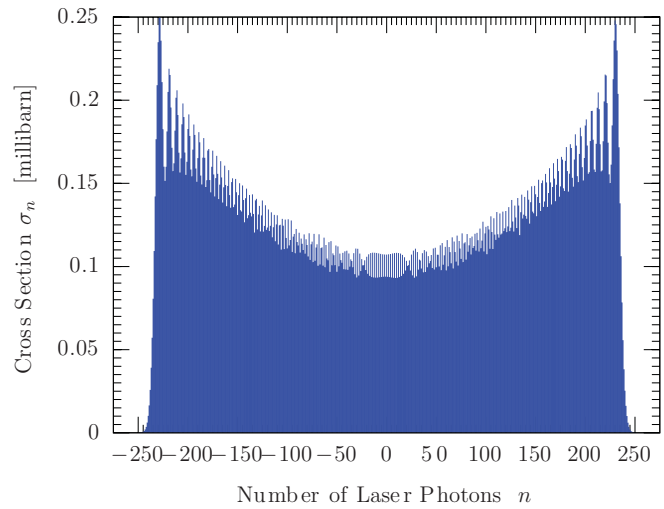

FIG. 2. (Color online) Same as Fig. 1, but for a laser frequency of $\omega_0 = 100$ eV at intensity $I = 6.25 \times 10^{21}$ W/cm^2.

moving freely in an external laser field of the form (2). The initial proton momentum outside the field is denoted as $\vec{p}$. Then the classical instantaneous energy of the proton in the field is

$$E_{\vec{p}}(t) = \frac{p^2}{2m} + U_\mathrm{p} - \frac{eA_0}{m}[p_1 \cos(\omega_0 t) + p_2 \sin(\omega_0 t)], \quad (29)$$

which shows an oscillatory temporal behavior. The amplitude of these oscillations is largest, when the proton momentum lies in the polarization plane of the laser field. Accordingly, the proton energy can vary within the boundaries

$$\frac{p^2}{2m} + U_\mathrm{p} - \frac{eF_0 p}{m\omega_0} \leqslant E_{\vec{p}}(t) \leqslant \frac{p^2}{2m} + U_\mathrm{p} + \frac{eF_0 p}{m\omega_0}, \quad (30)$$

resulting in an energetic width of $\Delta E = 2eF_0 p/(m\omega_0)$. The same width of the distribution of photo-proton energies $E_n = \omega_\gamma + n\omega_0 - U_\mathrm{p} - E_b$ results in the quantum description of the process. There, it follows from the maximum number of laser photons involved in the process, which is given by $n_\mathrm{max} \approx \alpha_\mathrm{max}$. The latter corresponds to a total laser photon energy of $n_\mathrm{max}\omega_0 \approx eF_0 p_\mathrm{max}/(m\omega_0)$, which is either absorbed from or emitted into the laser field.

Concluding this section, we point out that a photo-proton energy spectrum with a total width of 40 keV as in Fig. 2 would also result from the assistance of an optical laser with a frequency of $\omega_0 = 2$ eV and an intensity of $I = 2.5 \times 10^{18}$ W/cm^2. Such field parameters are available today from powerful tabletop laser systems. While the general appearance of the proton spectrum will be similar to the one in Fig. 2, its numerical calculation is substantially more involved due to the very large number $n \sim 10^4$ of laser photons participating in the process.

C. Dependence on field geometry

Finally, we address the question of how the relative orientation of the laser field with respect to the polarization direction of the γ photon influences the proton emission. So far we have considered the situation where the γ-photon polarization vector lies in the polarization plane of the circularly polarized laser field [in the notation of Eqs. (2) and (4), $\vec{e}_1 = \vec{e}_y$, $\vec{e}_2 = \vec{\varepsilon} = \vec{e}_z$]. Figure 3(a) shows a corresponding distribution of the partial cross sections σ_n for a laser frequency of $\omega_0 = 200$ eV and a laser intensity of 6.25×10^{21} W/cm^2. It extends over an energetic width from about 2.85 MeV to 2.87 MeV.

In contrast, when the γ-photon polarization is perpendicular to the polarization plane of the laser ($\vec{e}_1 = \vec{e}_x$, $\vec{e}_2 = \vec{e}_y$, $\vec{\varepsilon} = \vec{e}_z$), with all other parameters remaining unchanged, the distribution in Fig. 3(b) results. While the total widths of both distributions are the same, their shapes are qualitatively different. The distribution in Fig. 3(a) exhibits a rich structure with maxima at the outer edges, as we have seen before in Sec. III B. Instead, for the field configuration of Fig. 3(b), the distribution possesses a smooth bell-shaped form with the maximum lying at the center.

The distinct dependence on the relative field orientation can be understood by noting the following points:

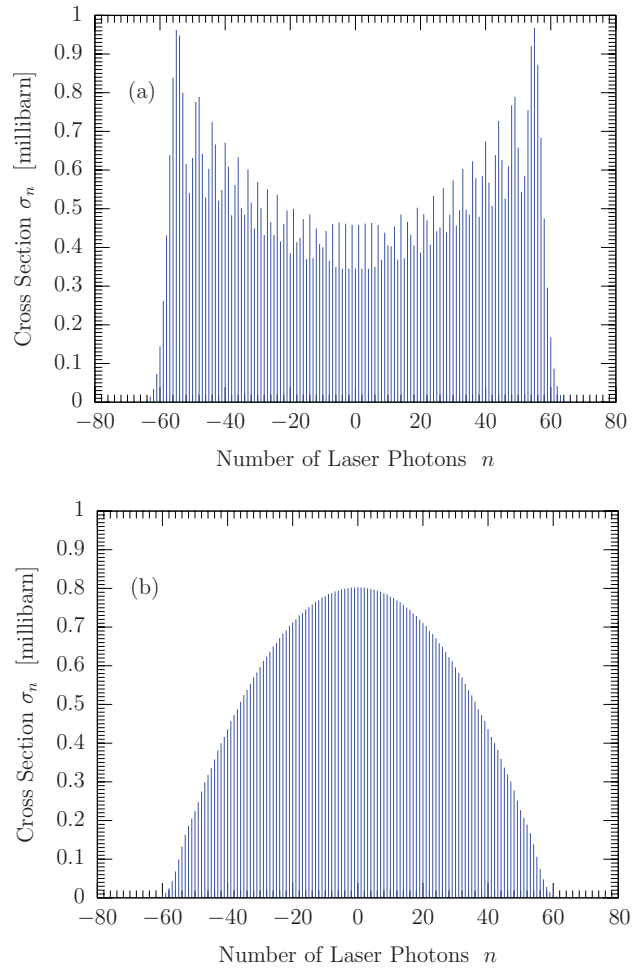

FIG. 3. (Color online) (a) Same as Fig. 1, but for laser frequency $\omega_0 = 200$ eV and laser intensity $I = 6.25 \times 10^{21}$ W/cm^2; (b) Same as (a) but the laser field is polarized in the x-y plane (i.e., perpendicularly to the polarization direction of the γ photon).

(i) from the usual photoeffect it is known that, in the nonrelativistic domain, the photo-proton is preferentially emitted under small angles around $\theta \approx 0$ with respect to the polarization direction of the γ photon [34];

(ii) the coupling strength between the proton and the laser field depends on the proton momentum component within the laser polarization plane [see Eq. (28)].

Therefore, in our notation, the majority of protons are emitted with a large momentum component p_z (as compared with p_x and p_y) and it matters whether this component lies inside or outside the polarization plane of the laser. When p_z lies inside the laser polarization plane, then the laser couples strongly to the proton and the Bessel function argument is, on average, large ($\alpha \propto \cos\theta$). This renders the emission or absorption of a large number of laser photons very likely, leading to the pronounced side wings in Fig. 3(a).

When, instead, the γ-photon polarization is perpendicular to the polarization plane of the laser, the laser-proton coupling is mediated through the relatively small momentum components p_x and p_y, so that the Bessel function argument is mostly small ($\alpha \propto \sin\theta$). As a consequence, it is more probable that

the proton emission proceeds with participation of only a small number of laser photons whereas high photon orders are suppressed [see Fig. 3(b)].

Before we proceed to the conclusion, we note that all calculations of Sec. III have also been performed by applying another form of the bound halo state in order to test the sensitivity of our predictions to the particular choice of the Yukawa wave function in Eq. (8). To this end, a hydrogenlike $2s$ state has been employed, which is often used to model the neutron halo in ^{11}Be [35]. Only very small differences were found. For instance, when the $2s$ state is used, the resulting total cross section deviates from the value given above by a few percent. Thus, the particular form of the bound halo wave function has only a minor influence on our results.

IV. CONCLUSION AND OUTLOOK

Photo-proton emission from halo nuclei subject to the combined fields of a γ photon and an intense, circularly polarized laser wave has been investigated. An S-matrix theory within the framework of the strong-field approximation as known from atomic physics was presented and applied to the laser-assisted photoeffect in ^{8}B. It was shown that the presence of the laser field may substantially influence the energy distribution of the emitted proton. The transition from perturbative to nonperturbative laser-proton interaction was illustrated and the fully nonperturbative regime was discussed. Here, the width of the energy distribution is determined by the maximum classical kinetic energy that the proton may gain (or lose) in the laser field. The width therefore scales with the amplitude of the laser vector potential. For the field parameters under consideration, the total cross section of the photo-proton emission is not affected by the presence of the laser field.

In summary, the laser-assisted nuclear photoeffect shares many similarities with its atomic-physics counterpart [20,21]. We emphasize that while our theory has been designed for application to one-proton halo nuclei, qualitatively similar effects can be expected for laser-assisted photo-proton emission from ordinary nuclei as well.

As an outlook, we note that further analogies between atomic and nuclear processes in strong laser fields may exist. For example, the inverse of the laser-assisted nuclear photoeffect would be radiative proton capture by a nucleus in the presence of a laser field. The corresponding process in atomic physics is laser-assisted radiative recombination of electrons with ions [22]. This process also represents the final step in high-harmonic generation from atoms or molecules in external laser fields [36]. At future high-intensity laser facilities, corresponding processes could be stimulated in nuclei as well. At optical laser intensities of $I \gtrsim 10^{24}$ W/cm^2 as envisaged at the Extreme Light Infrastructure [6], the laser-driven proton dynamics would even become relativistic.

ACKNOWLEDGMENTS

Valuable input by K. Z. Hatsagortsyan is gratefully acknowledged. We also thank W. Nörtershäuser for useful conversations on halo nuclei. A.D. acknowledges support from the International Max Planck Research School for Quantum Dynamics in Physics, Chemistry and Biology (IMPRS-QD).

[1] J. Chadwick and M. Goldhaber, Nature (London) **134**, 237 (1934).
[2] W. Bothe and W. Gentner, Z. Phys. **106**, 236 (1937); **112**, 45 (1939).
[3] See, e.g., Y. Assafiri *et al*., Phys. Rev. Lett. **90**, 222001 (2003); C. Nair *et al*., Phys. Rev. C **78**, 055802 (2008); R. Röhlsberger, K. Schlage, B. Sahoo, S. Couet, and R. Rüffer, Science **328**, 1248 (2010).
[4] K. W. D. Ledingham, P. McKenna, and R. P. Singhal, Science **300**, 1107 (2003); D. Umstadter, J. Phys. D **36**, 151R (2003); K. W. D. Ledingham and W. Galster, New J. Phys. **12**, 045005 (2010).
[5] N. V. Zamfir, D. Habs, F. Negoita, and D. Ursescu, Proc. SPIE **8080**, 80800X (2011).
[6] For current information, see [http://www.eli-np.ro].
[7] S. Matinyan, Phys. Rep. **298**, 199 (1998).
[8] G. Pretzler *et al*., Phys. Rev. E **58**, 1165 (1998); T. Ditmire *et al*., Nature (London) **398**, 489 (1999).
[9] K. W. D. Ledingham *et al*., Phys. Rev. Lett. **84**, 899 (2000); T. E. Cowan *et al*., *ibid*. **84**, 903 (2000); H. Schwoerer, P. Gibbon, S. Düsterer, R. Behrens, C. Ziener, C. Reich, and R. Sauerbrey, *ibid*. **86**, 2317 (2001).
[10] P. Kálmán and J. Bergou, Phys. Rev. C **34**, 1024 (1986); P. Kálmán, *ibid*. **39**, 2452 (1989); D. Kis, P. Kálmán, T. Keszthelyi, and J. Szívós, Phys. Rev. A **81**, 013421 (2010).
[11] P. Kálmán and T. Keszthelyi, Phys. Rev. A **47**, 1320 (1993); S. Typel and C. Leclercq-Willain, *ibid*. **53**, 2547 (1996).
[12] J. C. Solem and L. C. Biedenharn, J. Quant. Spectrosc. Radiat. Transfer **40**, 707 (1988); J. F. Berger, D. M. Gogny, and M. S. Weiss, Phys. Rev. A **43**, 455 (1991); F. X. Hartmann, D. W. Noid, and Y. Y. Sharon, *ibid*. **44**, 3210 (1991); N. Milosevic, P. B. Corkum, and T. Brabec, Phys. Rev. Lett. **92**, 013002 (2004); A. S. Kornev and B. A. Zon, Laser Phys. Lett. **4**, 588 (2007); A. Shahbaz, C. Müller, T. J. Bürvenich, and C. H. Keitel, Nucl. Phys. A **821**, 106 (2009).
[13] D. Habs, T. Tajima, J. Schreiber, C. P. J. Barty, M. Fujiwara, and P. G. Thirolf, Eur. Phys. J. D **55**, 279 (2009).
[14] T. J. Bürvenich, J. Evers, and C. H. Keitel, Phys. Rev. Lett. **96**, 142501 (2006); W.-T. Liao, A. Pálffy, and C. H. Keitel, Phys. Lett. B **705**, 134 (2011).
[15] T. J. Bürvenich, J. Evers, and C. H. Keitel, Phys. Rev. C **74**, 044601 (2006).
[16] H. A. Weidenmüller, Phys. Rev. Lett. **106**, 122502 (2011)
[17] F. Ehlotzky, K. Krajewska, and J. Z. Kamiński, Rep. Prog. Phys. **72**, 046401 (2009).
[18] T. Kirchner, Phys. Rev. Lett. **89**, 093203 (2002); E. Lötstedt, U. D. Jentschura, and C. H. Keitel, *ibid*. **101**, 203001 (2008); A. B. Voitkiv, B. Najjari, and J. Ullrich, *ibid*. **103**, 193201 (2009); R. Kanya, Y. Morimoto, and K. Yamanouchi, *ibid*. **105**, 123202 (2010); H. M. Castañeda Cortés, S. V. Popruzhenko, D. Bauer, and A. Pálffy, New J. Phys. **13**, 063007 (2011).

[19] A. B. Voitkiv, N. Grün, and J. Ullrich, J. Phys. B **36**, 1907 (2003).
[20] See, e.g., P. Kálmán, Phys. Rev. A **38**, 5458 (1988); C. Leone, S. Bivona, R. Burlon, and G. Ferrante, *ibid.* **38**, 5642 (1988); V. Véniard, R. Taïeb, and A. Maquet, Phys. Rev. Lett. **74**, 4161 (1995); D. B. Milošević and F. Ehlotzky, Phys. Rev. A **57**, 2859 (1998); C. Buth and R. Santra, *ibid.* **75**, 033412 (2007); A. K. Kazansky, A. V. Grigorieva, and N. M. Kabachnik, Phys. Rev. Lett. **107**, 253002 (2011).
[21] T. E. Glover, R. W. Schoenlein, A. H. Chin, and C. V. Shank, Phys. Rev. Lett. **76**, 2468 (1996); P. Johnsson *et al.*, *ibid.* **95**, 013001 (2005); M. Meyer *et al.*, *ibid.* **101**, 193002 (2008); K. Klünder *et al.*, *ibid.* **106**, 143002 (2011).
[22] See, e.g., J. Z. Kamiński and F. Ehlotzky, J. Mod. Opt. **50**, 621 (2003); C. Müller, A. B. Voitkiv, and B. Najjari, J. Phys. B **42**, 221001 (2009).
[23] T. Minamisono *et al.*, Phys. Rev. Lett. **69**, 2058 (1992); L. Trache, F. Carstoiu, C. A. Gagliardi, and R. E. Tribble, *ibid.* **87**, 271102 (2001); D. Cortina-Gil *et al.*, Phys. Lett. B **529**, 36 (2002); Nucl. Phys. A **720**, 3 (2003); T. Sumikama *et al.*, Phys. Rev. C **74**, 024327 (2006).
[24] M. Fukuda *et al.*, Nucl. Phys. A **656**, 209 (1999).
[25] M. H. Smedberg *et al.*, Phys Lett. B **452**, 1 (1999).
[26] For other types of halo nuclei, we refer to R. K. Gupta, S. Kumar, M. Balasubramaniam, G. Münzenberg, and W. Scheid, J. Phys. G **28**, 699 (2002); W. Geithner *et al.*, Phys. Rev. Lett. **101**, 252502 (2008); W. Nörtershäuser *et al.*, *ibid.* **102**, 062503 (2009).
[27] S. S. Chandel, S. K. Dhiman, and R. Shyam, Phys. Rev. C **68**, 054320 (2003).
[28] M. Abramowitz and I. A. Stegun, *Handbook of Mathematical Functions* (Dover, New York, 1965).
[29] A. Giulietti *et al.*, Phys. Rev. Lett. **101**, 105002 (2008).
[30] W. Ackermann *et al.*, Nature Photon. **1**, 336 (2007); for current information, see [http://flash.desy.de].
[31] L. Young *et al.*, Nature (London) **466**, 56 (2010); for current information, see [http://lcls.slac.stanford.edu].
[32] A. Pukhov, Nature Phys. **2**, 439 (2006); B. Dromey *et al.*, *ibid.* **5**, 146 (2009)
[33] H. R. Reiss, J. Math. Phys. **3**, 387 (1962); Eur. Phys. J. D **55**, 365 (2009).
[34] V. B. Berestetskii, E. M. Lifshitz, and L. P. Pitaevskii, *Relativistiv Quantum Theory* (Pergamon, New York, 1971).
[35] See, e.g., M. S. Hussein, A. F. R. de Toledo Piza, O. K. Vorov, and A. K. Kerman, Phys. Rev. C **60**, 064615 (1999).
[36] M. Klaiber, K. Z. Hatsagortsyan, C. Müller, and C. H. Keitel, Opt. Lett. **33**, 411 (2008); for an upcoming review, see M. C. Kohler, T. Pfeifer, K. Z. Hatsagortsyan, and C. H. Keitel, arXiv:1201.5094.